



HAL
open science

Investigation of the thermodynamic properties of Al₄C₃: A combined DFT and DSC study

A. Pisch, A. Pasturel, G. Deffrennes, O. Dezellus, P. Benigni, G. Mikaelian

► To cite this version:

A. Pisch, A. Pasturel, G. Deffrennes, O. Dezellus, P. Benigni, et al.. Investigation of the thermodynamic properties of Al₄C₃: A combined DFT and DSC study. *Computational Materials Science*, 2020, 171, pp.109100. 10.1016/j.commatsci.2019.109100 . hal-02317849

HAL Id: hal-02317849

<https://hal.science/hal-02317849>

Submitted on 28 Nov 2019

HAL is a multi-disciplinary open access archive for the deposit and dissemination of scientific research documents, whether they are published or not. The documents may come from teaching and research institutions in France or abroad, or from public or private research centers.

L'archive ouverte pluridisciplinaire **HAL**, est destinée au dépôt et à la diffusion de documents scientifiques de niveau recherche, publiés ou non, émanant des établissements d'enseignement et de recherche français ou étrangers, des laboratoires publics ou privés.

1 Investigation of the thermodynamic properties of Al_4C_3 : a combined
2 DFT and DSC study.

3
4 A. Pisch*, A. Pasturel

5 Univ. Grenoble Alpes, CNRS, Grenoble INP, SIMaP, F-38000 Grenoble, France

6 G. Deffrennes, O. Dezellus

7 Laboratoire des Multimatériaux et Interfaces, Université Claude Bernard Lyon 1, F-69622

8 Villeurbanne, France.

9 P. Benigni, G. Mikaelian

10 Aix Marseille Univ, Université de Toulon, CNRS, IM2NP, F-13397 Marseille, France

11 * corresponding author: alexander.pisch@simap.grenoble-inp.fr

12

13 Abstract

14 The question of material stability through the determination of the thermodynamic properties is of
15 fundamental and technological importance to any analysis of system properties in many applications.

16 For Al_4C_3 , its experimental heat of formation varies widely, from -0.187 to -0.363 eV/atom, which

17 makes it difficult to use such experimental information for any reactivity assessment. Here, we

18 demonstrate that density functional theory (DFT), with the recently developed strongly constrained

19 and appropriately normed (SCAN) functional, is especially powerful in critically assessing these

20 experimental data. In order to have a more complete description of thermodynamic properties of

21 Al_4C_3 , we also determine the temperature dependence of its heat capacity using both the harmonic

22 and quasi-harmonic approximation. In addition, and to select the most efficient approximation, we

23 come back to the experimental background by using differential scanning calorimetry (DSC) to

24 measure this quantity at constant pressure up to very high temperatures, namely 850K.

25 Keywords: Aluminum Carbide; Thermodynamic properties; DFT; SCAN+vdW functional

26 1. Introduction

27

28 Aluminum Carbide is a refractory material with applications in various technical fields. It is a potential
29 stable phase in the carbothermic reduction of alumina [1]. It may be a product in the reaction of
30 aluminum with silicon carbide [2]. Al_4C_3 is also present in selected composite ceramics in the Y-Al-Si-
31 C-O system [3]. In addition, Al_4C_3 is an important phase for Al-based metal matrix composites.
32 Recently, some authors reported its use as reinforcement [4–6]. However, the formation of Al_4C_3 is
33 most widely associated with a severe degradation of properties of composites [7,8]. For instance,
34 Al_4C_3 might form at the matrix/reinforcement interface during processing, dissolving the
35 reinforcements and causing embrittlement. Last but not least, Al_4C_3 is a semiconducting material and
36 can be used in electronic components such as diodes [9].

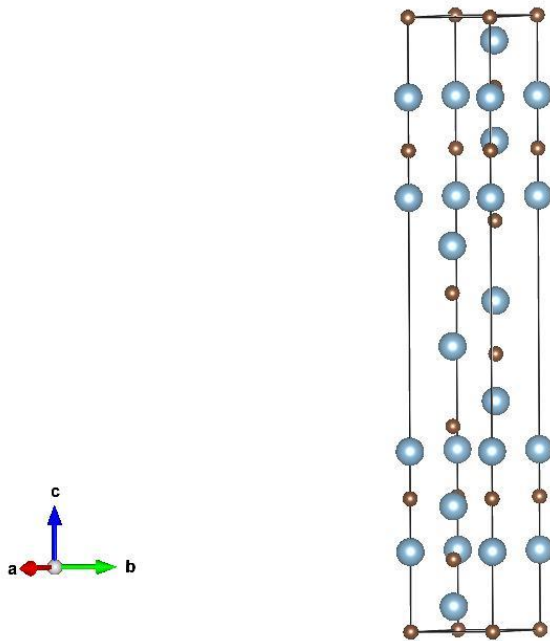
37 In order to control the stability of the phase and the synthesis conditions, a thorough knowledge of
38 the thermodynamic properties of solid Al_4C_3 is mandatory. Its heat of formation, heat capacity at
39 constant pressure and Gibbs energy were then studied intensively over the last 120 years but
40 surprisingly the reported experimental values display large discrepancies. Indeed the standard heat
41 of formation obtained from different experimental techniques involving variety of calorimetric
42 methods based on combustion, acid-solution and direct-reaction and 2nd / 3rd law analysis of vapor
43 pressure measurements [10–21] display a large range of values, varying from -0.187 to -0.363
44 eV/atom.

45 More recently, DFT is applied as a computationally efficient component of a methodology capable of
46 accurately determining structural properties and energies of formation of many compounds.

47 Furthermore, this methodology should also be used where experimental data are lacking, i.e. in the
48 prediction of new materials or in the case of experimental discrepancies or controversies. DFT with
49 the PBE [22] generalized gradient approximation (GGA) to its exchange-correlation energy is the
50 most common approach due to its relatively cheap computational cost and reasonable accuracy.

51 However, the theoretical determination at 0K of the heat of formation of Al_4C_3 using this

52 approximation [23] is considerably less negative than all experimental values, namely -0.013
53 eV/atom, preventing any use of theory to critically assess the experimental data. Note that
54 corrections to include thermal contributions at T=298K [24,25] yields a value of -0.015 eV/atom but
55 do not change the previous conclusion. Such a discrepancy can be attributed to the use of PBE, a
56 common deficiency found in DFT calculations to capture the cohesive energy of graphite accurately
57 [26]. The absence of van der Waals (vdW) interactions in PBE is the major source of error to describe
58 the layered structure of graphite. We also emphasize that Al_4C_3 has an unusual crystal structure that
59 consists of alternating layers of Al_2C and Al_2C_2 (see Fig. 1) and PBE seems not to be accurate enough
60 to describe its structural and cohesive properties.



61

62 Figure 1: Crystal structure of Al_4C_3

63 In this work, we investigate the structural and thermodynamic properties of Al_4C_3 using the recent
64 SCAN many-body interaction functional [27]. First, we find that SCAN significantly improves the
65 agreement between the experimental and calculated ground state properties of C-graphite and
66 those of Al_4C_3 . As a consequence, the energy of formation of Al_4C_3 at 0K is -0.236 eV/atom, a value
67 that is now located inside the range of experimental values. Moreover, we complete our theoretical

68 analysis at $T = 0\text{K}$ by including temperature effects through the calculation of the temperature
69 dependence of the heat of capacity of Al_4C_3 as well as those of Al-fcc and C-graphite. Both harmonic
70 and quasi-harmonic approximations are tested to determine these temperature dependences. Using
71 the quasi-harmonic approximation, we obtain a standard heat of formation equal to -0.250 eV/atom .
72 As experimental heat capacity data of Al_4C_3 are only available at temperatures below 350K , we also
73 determine its temperature dependence up to 850K by using the “discontinuous method” as
74 described by Höhne et al. [28]. This experimental study allows to identify that the quasi-harmonic
75 approximation provides theoretical values in close agreement with experimental data up to 500K .

76 2. Theoretical and experimental details

77 2.1. DFT calculations

78

79 The ground state properties of pure carbon (graphite, diamond), aluminum (fcc) and Al_4C_3 were
80 calculated using density functional theory DFT [29,30] and the VASP software package [31,32] in its
81 most recent version (5.4.4).

82 The Strongly Conditioned and Appropriately Normed (SCAN) semi-local density functional [27] was
83 chosen for the calculations. In addition, we include van der Waals interactions to take into account
84 the long range order phenomena in these carbon based materials. The numerical routines from
85 Klimes et al. [33,34] as implemented in the VASP code were used. For Al, the 3p and 3s orbitals and
86 for C, the 2p and 2s orbitals are considered as valence states in the calculations. The energy cutoff for
87 the projector augmented plane-wave bases was set to 800 eV . An automatically generated, gamma
88 centered grid of k-points in the irreducible part of the Brillouin zone was used following the
89 Monkhorst-Pack scheme [35].

90 The lattice parameters of all compounds as well as their internal atomic coordinates were fully
91 relaxed. The linear tetrahedron method with Blöchl corrections [36] was used to calculate the
92 electronic density of states (DOS) for C-graphite and diamond as well as for Al_4C_3 . For Al-fcc, the

93 Methfessel-Paxton method of 2nd order was used for the relaxation calculation. All relaxations were
94 performed with a convergence criterion of 10⁻⁸ eV/Å for the total energy.

95 Zero Point Energy (ZPE) and heat capacities at constant volume / pressure to access finite
96 temperature properties can be obtained from lattice dynamics theory. The phonon spectra of all
97 compounds were calculated with the frozen phonon (supercell) method using the phonopy code [37]
98 coupled to VASP. The generated supercells for the different compounds were: 5x5x2 for C-graphite,
99 3x3x3 for C-diamond and Al-fcc and 2x2x1 for Al₄C₃. The convergence criteria for the Hellman-
100 Feynman forces was set to 10⁻⁶ eV/Å to avoid any kind of residual strain in the lattice.

101 [2.2 Experimental study](#)

102

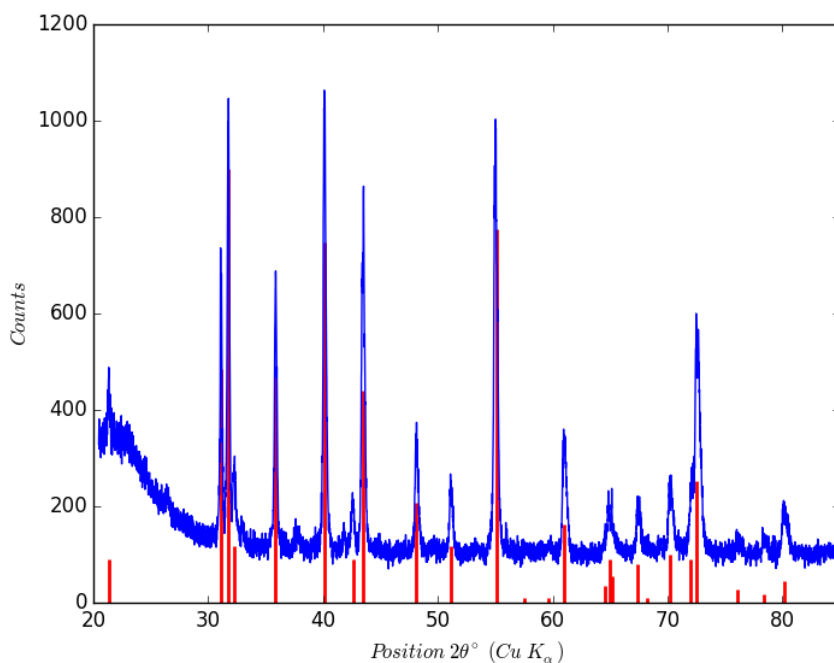
103 Al₄C₃ powder was purchased from the Alfa Aesar company. The chemical analysis obtained from the
104 manufacturer is shown in Table 1. As this product is moisture sensitive, the as received bottle
105 containing the carbide powder was opened and further handled in a glove box maintained under a
106 protective atmosphere of purified argon (O₂ < 10 ppm, H₂O < 5 ppm).

107 Table 1. Characteristics of the Al₄C₃ powder according to Alfa Aesar's datasheet, in wt.% .

Product No	14038
Purity	99 %+ metals basis
Lot No	X22B028
C total	24.6 %
Al	72.0 %
Fe	0.1 %
N	0.8 %
O	1.4 %

108

109 The as received carbide powder was first analyzed by XRD. To avoid any potential hydration of the
110 product during the XRD analysis, the aluminum carbide powder was loaded within the glovebox, in
111 an airtight specimen holder equipped with a dome like X-ray transparent cap. During the specimen
112 holder filling, it was not possible to perfectly flatten the surface of the powder because of the risk to
113 trap powder grains in the groove of the O-ring of the holder, which could jeopardize the air-
114 tightness. The specimen holder was then transferred to the diffractometer equipped with a copper
115 anode and analyzed in the [20-85°] 2θ range, with a step size of 0.013° and a scan step time of 196.7
116 s. The experimental diffractogram is compared in Figure 1 to the powder data file 00-035-0799
117 reference pattern of the Al₄C₃ aluminum carbide calculated for the copper K(α) wavelength. An
118 angular correction has been applied to the experimental diffractogram to take into account a slight
119 difference between the z position of the powder diffracting surface and the 2θ rotation axis of the
120 goniometer. As already mentioned above, impossibility to level the powder surface during holder
121 filling is the main reason explaining the necessity of this correction.



122
123 Figure 2: Corrected diffractogram of the as received Al₄C₃ powder compared to the 00-035-0799
124 reference pattern of Al₄C₃.

125 The low angles ($2\theta < 30^\circ$) broad peak is due to the x-ray scattering by the glassy specimen holder
126 dome. There is a good match between the diffractogram of the tested powder and the reference
127 pattern both in term of peak positions and intensities. Moreover, even if some few and low intensity
128 additional peak can be observed, no secondary phases can be detected on the diffractogram.
129 Therefore, the amount of secondary phases can be considered to be lower than 1 wt.%.

130 The heat capacity was measured by the so-called “small temperature steps procedure” or
131 “discontinuous method” using the classical three steps method as described by Höhne et al. [28].
132 with a DSC 111 calorimeter from the Setaram Company. Further details on the calorimeter and on
133 the experimental protocol can be found in Benigni et al. [38]. Four stainless steel crucibles provided
134 by Setaram were used in the experiments. The crucibles were sealed with a crimping tool inside the
135 glovebox. The first crucible was filled with 132.98 mg of Al_4C_3 , the second with 133.571 mg of
136 Standard Reference Material 720 $\alpha\text{-Al}_2\text{O}_3$ [39], the other two were sealed empty. The temperature
137 program and the processing of the recorded thermograms were performed with the SETSOFT 2000
138 software provided by Setaram. The parameters in the temperature program were set as follows: 2.5
139 K temperature step, 1.5 K/min heating rate between each step, and 800 s stabilization time after
140 each step. The heat capacity was measured between 300 and 873 K. A point by point correction
141 factor calculated from the ratio between the reference [39] and the apparent heat capacity of $\alpha\text{-}$
142 Al_2O_3 was applied. The uncertainty of the heat capacity measurements is estimated to be around
143 $\pm 2.5\%$ [38].

144 3. Results and Discussion:

145 3.1. Structural and cohesive properties of C-graphite and C-diamond

146

147 The crystal structure of hexagonal C-graphite was determined by Nelson & Riley [40], Baskin & Meyer
148 [41], Trucano & Chen [42], Zhao & Spain [43] and Howe et al. [44]. It crystallizes in the $\text{P6}_3\text{mmc}$ space
149 group with two fixed atomic positions: C1 (0 0 $1/4$) and C2 ($1/3$ $2/3$ $1/4$). C-diamond crystallizes in the
150 cubic $\text{Fd-}3\text{m}$ structure. Lattice parameter studies were performed by Riley [45], Straumanis & Aka

151 [46] and Hom et al. [47]. DFT calculations of the two allotropes of carbon were also performed using
 152 PBE [23]. While the agreement for C-diamond is good, the agreement for C-graphite is poor,
 153 especially the calculated c-axis is much longer than the experimental one. As already discussed in the
 154 introduction, the absence of vdW interactions in PBE does not allow to reproduce the interlayer
 155 coupling in the C-graphite structure. Note this remark holds also for other layered materials [26].

156 The available experimental [40–47] and theoretical [23,48,49] structural data for C-graphite and C-
 157 diamond are reported in Table 2 together with our values of the lattice constants obtained from
 158 SCAN calculations including vdW interactions. In the following we will use the term SCAN when
 159 referring to our findings. For C-graphite, the agreement with the low temperature data from Baskin
 160 & Meyer [41] is excellent. The c-axis elongation, as observed using PBE, disappears with SCAN. This
 161 confirms that the SCAN functional is particularly adapted describe the electronic properties of
 162 layered materials such as C-graphite. For C-diamond, an excellent agreement between the calculated
 163 and measured lattice parameters is also observed whatever the functional.

164 Table 2: Lattice parameters and cell volumes for C-graphite and C-diamond.

		a [Å]	c[Å]	V [Å ³]	Temperature	Reference
C-graphite	Experimental	2.4612	6.7079	35.189	285K	Nelson & Riley [40]
		2.4579	6.6720		4.2K	Baskin & Meyer [41]
		2.4589	6.7076		297K	
		2.464(2)	6.711(4)	35.294	300K	Trucano & Chen [42]
		2.462	6.707	35.207	298K	Zhao & Spain [43]
		2.4617(2)	6.7106(4)	35.219	298K	Howe et al. [44]
	Calculated	2.482	6.60		0K	LCAO, Zunger [48]
		2.468	8.685	45.803	0K	PBE, Jain et al. [23]
		2.450	6.670	34.673	0K	SCAN [This work]

C-diamond	Experimental	3.56679		45.377	298K	Riley [45]
		3.56684		45.379	293K	Straumanis & Aka [46]
		3.566986		45.384	298K	Hom et al. [47]
	Calculated	3.602		46.734	0K	LMTO, Yin & Cohen [49]
		3.574		45.652	0K	PBE, Jain et al. [23]
		3.551		44.777	0K	SCAN [This work]

165

166 In Table 3, we compare the cohesive energy of C-graphite and C-diamond computed at T=0K using
 167 both PBE and SCAN functionals with the experimental data [50].

168 Table 3: Cohesive energy (in eV/atom) for C-graphite and C-diamond

	E_{coh} (PBE)	E_{coh} (SCAN)	E_{coh} (Exp.) [50]
C-diamond	7.737	7.456	7.361
C-graphite	7.860	7.610	7.374

169

170 From Table 3, we can see that PBE cohesive energies are significantly larger than the experimental
 171 values in both graphite and diamond while this overestimation is corrected by SCAN.

172 3.2 Structural properties of Al_4C_3 :

173

174 The first determination of the crystal structure of Al_4C_3 was performed by v. Stackelberg and
 175 Schnorrenberg in 1934 [51]. Al_4C_3 crystallizes in the R-3m space group (166). This was confirmed by
 176 Cox and Pidgeon [52] using powder diffraction. The structure was further refined by Jeffrey et al. [53]
 177 and more recently by Gesing and Jeitschko [54] using single crystals. The experimental lattice
 178 parameters and the atomic positions are summed up in Table 3a and 3b.

179 Table 3a: experimental and calculated lattice parameters and cell volume for Al₄C₃ in the hexagonal
 180 setting (R-3m space group)

	a [Å]	c [Å]	V [Å ³]	Temperature	Reference
Experimental	3.325	24.94	238.79	298K	v. Stackelberg & Schnorrenberg [51]
	3.30	24.89	234.74	298K	Jeffrey et al. [53]
	3.3355(1)	24.967(3)	240.56	298K	Gesing and Jeitschko [54]
Calculated	3.352	25.104	244.28	0K	PBE, Suetin et al. [55]
	3.354	25.117	244.69	0K	PBE, Jain et al. [23]
	3.335	24.967	240.50	0K	PBE, Sun et al. [56]
	3.3256	24.844	237.95	0K	SCAN [This work]

181

182 Table 3b: Experimental and calculated atomic positions for Al₄C₃ in the hexagonal setting

	Al I 6c	Al II 6c	C I 3a	C II 6c	Reference
Experimental	0 0 0.2916	0 0 0.1250	0 0 0	0 0 0.2291	v. Stackelberg & Schnorrenberg [51]
	0 0 0.296	0 0 0.129	0 0 0	0 0 0.217	Jeffrey et al. [53]
	0 0 0.29422(6)	0 0 0.12967(7)	0 0 0	0 0 0.2168(2)	Gesing and Jeitschko [54]
Calculated	0 0 0.29349	0 0 0.12990	0 0 0	0 0 0.21674	PBE, Jain et al. [23]
	0 0 0.29352	0 0 0.13016	0 0 0	0 0 0.21672	SCAN [This work]

183

184 DFT calculations using PBE were performed by Suetin et al. [55], Sun et al. [56] and in the frame of
 185 the materialsproject.org initiative [23]. We also report results obtained using SCAN. We note that

186 SCAN improves slightly structural values with respect to PBE and the agreement between DFT
187 calculations and experimental values is satisfactory. Again, the improvement mainly concerns the c-
188 axis length which is closer to the experimentally observed value when using SCAN.

189 3.3 Heat of formation and heat of capacity of Al_4C_3

190

191 The formation energy of Al_4C_3 at 0K is obtained by subtracting the weighed sum of the total energy of
192 constituting elements from the total energy of the compound:

$$193 \quad \Delta H = E_T(Al_4C_3) - 4/7E_T(Al) - 3/7E_T(C).$$

194 This formation energy is then corrected with respect to the Zero Point Energies (ZPE) estimated from
195 the frequency integration over the vibrational density of states [37]:

$$196 \quad \Delta H^{corr}(Al_4C_3) = \Delta H(Al_4C_3) + \Delta ZPE(Al_4C_3)$$

197 for which the ZPE correction is calculated as follows:

$$198 \quad \Delta ZPE = ZPE(Al_4C_3) - 4/7ZPE(Al) - 3/7ZPE(C)$$

199 The heat capacity at constant volume can be determined from the calculated Helmholtz free energy
200 F in the harmonic approximation (HA) using the vibrational density of states as a function of
201 frequency q of the band s:

$$202 \quad F(V_0, T) = \frac{1}{2} \sum_{q,s} \hbar \omega(q, s) + k_B T \sum_{q,s} \ln \left[1 - \exp \left(\frac{-\hbar \omega(q, s)}{k_B T} \right) \right]$$

203 The vibrational entropy and the heat capacity at constant volume are then given by:

$$204 \quad S = - \left(\frac{\partial F}{\partial T} \right)_V ; C_V = -T \left(\frac{\partial^2 F}{\partial T^2} \right)_V$$

205 When repeating the HA calculations at several different volumes V to obtain a minimum value of
206 $F(V, T)$, the heat capacity at constant pressure in the quasi-harmonic approximation, QHA, is obtained
207 from:

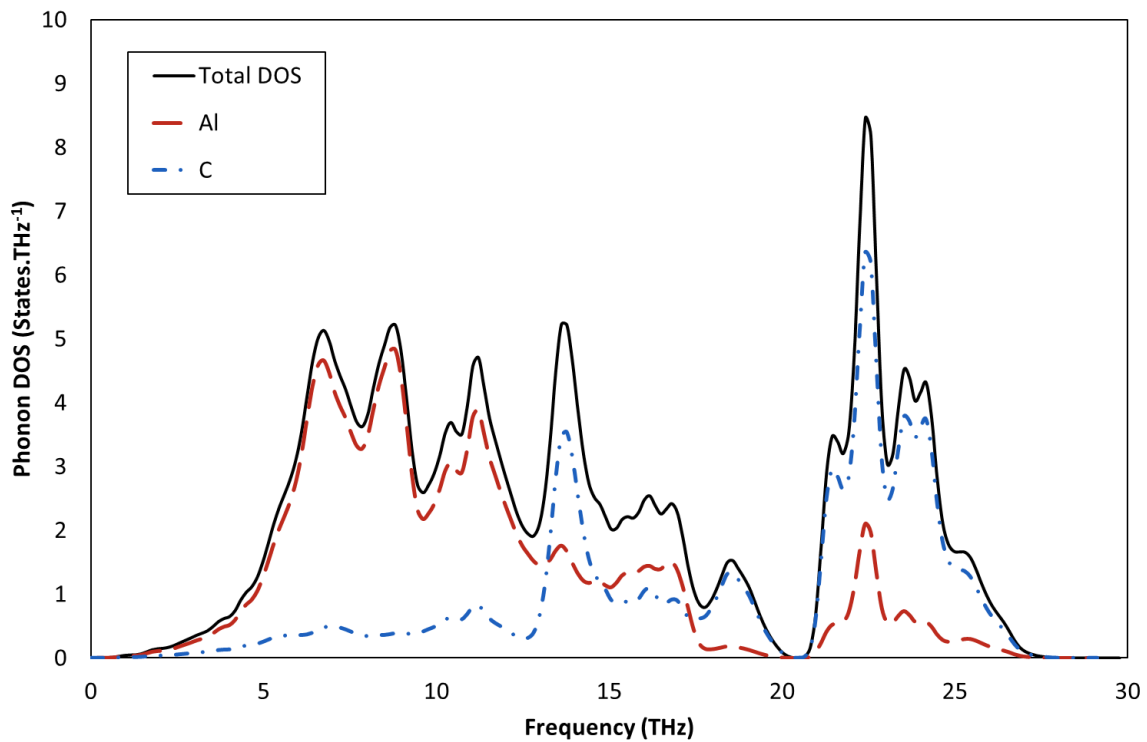
208
$$C_p = -T \left(\frac{\partial^2 G(T, P)}{\partial T^2} \right)$$

209 with $G(T, P) = \min_v [E(V) + F(V; T) + PV]$.

210 The standard heat of formation at 298K of Al_4C_3 is then obtained from 0K calculations by including
 211 the ZPE correction and by subtracting the weighed sum of the heat content of constituting elements
 212 from the heat content of the compound, namely $\Delta H_{0K}^{298K} = \Delta H_{0K}^{298K}(Al_4C_3) - 4/7\Delta H_{0K}^{298K}(Al) -$
 213 $3/7\Delta H_{0K}^{298K}(C)$.

214 In Figure 3 we present the calculated phonon Density of States (DOS) of Al_4C_3 used to determine the
 215 temperature dependence of its thermodynamic properties.

216

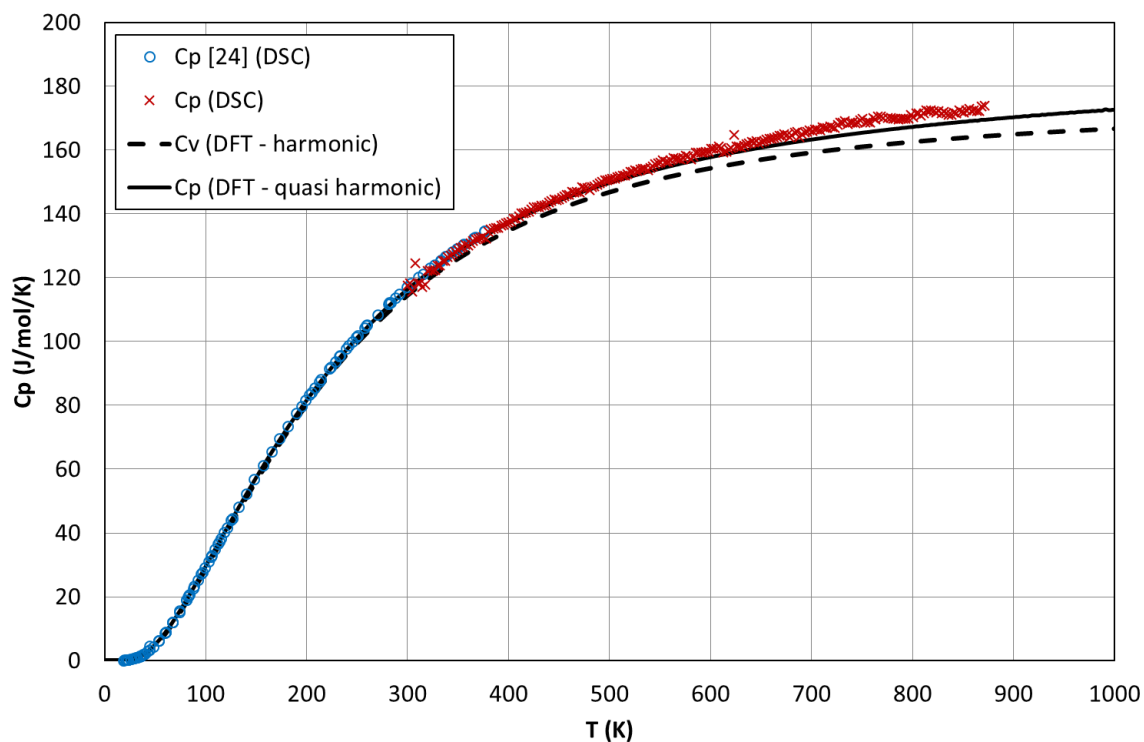


217

218 Fig.3: Calculated phonon Density of States (DOS) of Al_4C_3

219

220 The derived heat capacity at constant volume (harmonic approximation) and at constant pressure
 221 (quasi-harmonic approximation) are plotted in Figure 4 together with the available experimental data
 222 (present contribution and data from[24]).



223

224 Fig.4: Comparison of calculated heat capacity at constant volume (harmonic) and constant pressure
 225 (quasi-harmonic) with experimental values (from this work and from [24])

226 The calculated heat capacity at constant pressure agrees well with the measured data from
 227 Furukawa et al. [24] and from the present experimental determination up to 500K. At higher
 228 temperatures, anharmonic contributions become more important and the measured values are
 229 higher than the calculated ones.

230 The calculated ground state energies for Al-fcc, C-graphite and Al_4C_3 with the SCAN functional are
 231 summed up in Table 4. Using the calculated Zero Point Energies (ZPE) and the heat contents from 0K
 232 to 298K, the standard heat of formation of Al_4C_3 is -0.250 eV/atom. Note that the value obtained at
 233 T=0K using SCAN, namely -0.236 eV/atom, is much more negative than that obtained with PBE, -
 234 0.092 eV/atom.

235

236

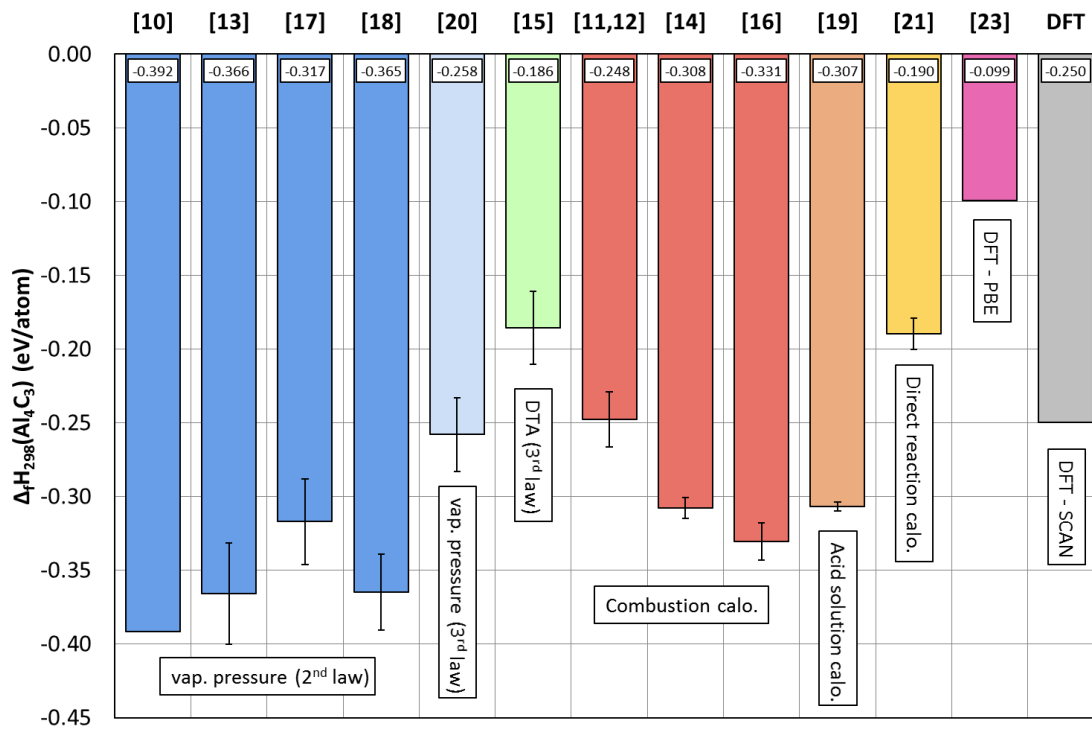
237

238 Table 4: Calculated ground state properties and derived heat of formation for solid Al₄C₃.

	E _T (0K) [eV/atom]	ZPE (0K) [eV/atom]	H(298K)-H(0K) [eV/atom]	ΔH(298K) [eV/atom]
Al-fcc	-7.699	0.037	0.047	
C-graphite	-10.052	0.175	0.011	
Al ₄ C ₃	-8.943	0.089	0.024	-0.250

239

240 The comparison of our calculated value with the literature information allows now a critical
 241 assessment of the available experimental data since the SCAN value is well located in the
 242 experimental range. To illustrate this, we report all the experimental data and our theoretical one in
 243 Figure 5. We find that the calculated standard heat of formation shows a good agreement with the
 244 calorimetric data from Meichsner & Roth [11,12] and Rinehart & Behrens [20] . All other values are
 245 considerably more or less exothermic than the calculated value, not to mention again the value using
 246 PBE [23] that is off the experimental range. Understanding the origin of the experimental
 247 discrepancies is beyond the scope of this work. However, incomplete reaction or metastable reaction
 248 products in the combustion or dissolution calorimetry experiments or kinetic blockage of the
 249 graphite layer at the sample surface during vaporization may explain the dispersion in experimental
 250 values obtained from vapor pressure measurements as indicated by Rinehart & Behrens [20].



251

252 Fig.5: Comparison of heat of formation of Al_4C_3 data from literature and this work

253 We can also use calculated heat capacity values from the quasi-harmonic approximation to

254 determine the standard entropy. We find a value of 0.924 meV/atom/K (89.12 J/mol/K), which is in

255 excellent agreement with the experimental one [24,57], i.e. 0.922 meV/atom/K (88.97 J/mol/K).

256 From the band structure of Al_4C_3 computed at $T=0\text{K}$, we obtain an indirect gap with a calculated value

257 of 1.342 eV which is equivalent to 1.315 eV using PBE [23]. It is important to mention that the use of

258 SCAN still underestimates band gap energies as this is generally the case for PBE [62].

259 Finally, there is a plausible additional correction in relation to the ground state properties of C-

260 graphite. The heat of reaction for the diamond to graphite transition in carbon was measured by

261 Rossini & Jessup [58] using combustion calorimetry and a value of $0.020 \pm 0.01 \text{ eV/atom}$ is reported at

262 298K. More recently, Kleppa and Hong [59] obtain a standard heat of reaction of 0.018 ± 0.010

263 eV/atom using high temperature solution calorimetry. In addition, Hultgren et al. [60] published an

264 assessed value of 0.020 eV/atom at 298K while in the compilation of Glushko [61], a value of

265 $0.019 \pm 0.01 \text{ eV/atom}$ is given. All these values are in close agreement. At 298K, the standard heat of

266 reaction calculated by SCAN including ZPE corrections and the heat content is equal to 0.070
267 eV/atom, as shown in Table 5.

268 Table 5: Calculated ground state properties of C-graphite and C-diamond using the SCAN
269 functional.

	E(0K) [eV/atom]	ZPE (0K) [eV/atom]	H(298K)-H(0K) [eV/atom]	$\Delta_r H(298K)$ [eV/atom]
C-graphite	-10.052	0.175	0.011	
C-diamond	-9.987	0.186	0.005	0.070

270

271 Then, we get a difference equal to 0.050 eV/atom between the experimental value obtained Rossini
272 & Jessup [58] and the calculated one. Note that the difference with PBE calculations is much more
273 important, namely 0.114 eV/atom.

274 If we attribute this difference to some limitations of SCAN in the accurate description of the ground
275 state properties of C-graphite as shown in Table 3, the heat of formation of Al_4C_3 has to be corrected
276 by a value equal to -0.022 eV/atom. The corrected value is then -0.272 eV/atom, which does not
277 modify our conclusions on the assessment of experimental values.

278 4. Conclusion

279

280 We have shown that the recently proposed SCAN functional including vdW interactions considerably
281 improves the theoretical prediction of the heat of formation of Al_4C_3 as well as the ground state
282 properties of C-graphite and C-diamond with respect to PBE calculations. We also demonstrated that
283 the calculated heat capacity at constant pressure using the quasi-harmonic approximation is in good
284 agreement with experimental data obtained by DSC up to 500K. Our theoretical approach is also
285 confirmed by the good agreement between the calculated standard entropy and the experimental
286 one. All these results allow us to critically assess the experimental heats of formation of Al_4C_3 which

287 is characterized by a wide range of available values using different experimental techniques. We thus
288 conclude that SCAN would provide an improved description of the thermodynamic properties of
289 layered materials more generally, at a cost comparable to PBE.

290 5. Acknowledgement

291
292 Fruitful discussions within the French collaborative network in high temperature thermodynamics
293 GDR CNRS n°3584 (TherMatHT) are acknowledged. Carine Perrin-Pellegrino (IM2NP) is gratefully
294 acknowledged for the XRD analysis of the Al₄C₃ powder.

295 6. Data availability

296
297 The raw/processed data required to reproduce these findings were added as supplementary
298 information.

299 7. References

- 300 [1] W.L. Worrell, Carbothermic Reduction of Alumina: A Thermodynamic Analysis, Canadian
301 Metallurgical Quarterly. 4 (1965) 87–95. doi:10.1179/cm.1965.4.1.87.
- 302 [2] L.L. Oden, R.A. McCune, Phase equilibria in the Al-Si-C system, Metallurgical Transactions A. 18
303 (1987) 2005–2014. doi:10.1007/BF02647073.
- 304 [3] J. Gröbner, Thermodynamische Berechnungen im System Y-Al-Si-C-O, University of Stuttgart,
305 Germany, 1994.
- 306 [4] M. Besterici, Preparation, microstructure and properties of Al–Al₄C₃ system produced by
307 mechanical alloying, Materials & Design. 27 (2006) 416–421.
308 doi:10.1016/j.matdes.2004.11.012.
- 309 [5] Y. Birol, Response to thermal exposure of the mechanically alloyed Al/C powder blends, Journal
310 of Alloys and Compounds. 460 (2008) L1–L5. doi:10.1016/j.jallcom.2007.05.071.
- 311 [6] M. Nagendra Naik, K. Dharma Reddy, P. Venkata Ramaiah, B. Venkata Narayana, G. Bhanodaya
312 Reddy, Exploration of Mechanical behaviour and Wear Behaviour of Al 4 C 3 Reinforced
313 Aluminium Metal Matrix Composites, Materials Today: Proceedings. 4 (2017) 2989–2998.
314 doi:10.1016/j.matpr.2017.02.181.
- 315 [7] M. Rodríguez-Reyes, M.I. Pech-Canul, J.C. Rendón-Angeles, J. López-Cuevas, Limiting the
316 development of Al₄C₃ to prevent degradation of Al/SiCp composites processed by pressureless
317 infiltration, Composites Science and Technology. 66 (2006) 1056–1062.
318 doi:10.1016/j.compscitech.2005.07.025.
- 319 [8] T. Etter, P. Schulz, M. Weber, J. Metz, M. Wimmmler, J.F. Löffler, P.J. Uggowitzer, Aluminium
320 carbide formation in interpenetrating graphite/aluminium composites, Materials Science and
321 Engineering: A. 448 (2007) 1–6. doi:10.1016/j.msea.2006.11.088.
- 322 [9] S.-M. Kim, S.-M. Koo, Electrical properties of Al/Al 4 C 3 /4H-SiC diodes, Materials Science in
323 Semiconductor Processing. 74 (2018) 170–174. doi:10.1016/j.mssp.2017.10.012.
- 324 [10] S. Satoh, The Heat of Formation and Specific Heat of Aluminium Carbide, Sc. Pap. I.P.C.R. 34
325 (1937) 50–59.

- 326 [11] A. Meichsner, W.A. Roth, Beiträge zur Thermochemie des Aluminiums, Ber. Bunsenges. Phys.
327 Chem. 40 (1934) 19–26.
- 328 [12] W.A. Roth, Die Bildungswärmen von Calciumaluminaten, Z. Elektrochemie. 48 (1942) 267.
- 329 [13] D.J. Meschi, A.W. Searcy, The Dissociation Pressure of Aluminum Carbide, The Journal of
330 Physical Chemistry. 63 (1959) 1175–1178. doi:10.1021/j150577a036.
- 331 [14] R.C. King, G.T. Armstrong, Heat of combustion and heat of formation of aluminum carbide,
332 Journal of Research of the National Bureau of Standards Section A: Physics and Chemistry. 68A
333 (1964) 661–668.
- 334 [15] W.J. Thoburn, Ph.D. Dissertation, University of Toronto, 1964.
- 335 [16] A.D. Mah, HEAT OF FORMATION OF ALUMINUM CARBIDE, U.S. Dept. of the Interior, Bureau of
336 Mines. (1964).
- 337 [17] E.R. Plante, C.H. Schreyer, Dissociation pressure of aluminum carbide using a rotating Knudsen
338 cell, Journal of Research of the National Bureau of Standards Section A: Physics and Chemistry.
339 70A (1966) 253.
- 340 [18] N.D. Potter, E. Murad, D.L. Hildenbrand, Y.H. Inani, W.F. Hall, Aeronutronic Publ. U-3748.
341 (1966).
- 342 [19] R.O.G. Blachnik, P. Gross, C. Hayman, Enthalpies of formation of the carbides of aluminium and
343 beryllium, Transactions of the Faraday Society. 66 (1970) 1058. doi:10.1039/tf9706601058.
- 344 [20] G.H. Rinehart, R.G. Behrens, Vaporization thermodynamics of aluminum carbide, The Journal of
345 Chemical Thermodynamics. 12 (1980) 205–215. doi:10.1016/0021-9614(80)90038-5.
- 346 [21] S.V. Meschel, O.J. Kleppa, Standard enthalpies of formation of AlB₁₂ and Al₄C₃ by high
347 temperature direct synthesis calorimetry, Journal of Alloys and Compounds. 227 (1995) 93–96.
348 doi:10.1016/0925-8388(95)01649-X.
- 349 [22] J.P. Perdew, K. Burke, M. Ernzerhof, Generalized Gradient Approximation Made Simple,
350 Physical Review Letters. 77 (1996) 3865–3868. doi:10.1103/PhysRevLett.77.3865.
- 351 [23] A. Jain, S.P. Ong, G. Hautier, W. Chen, W.D. Richards, S. Dacek, S. Cholia, D. Gunter, D. Skinner,
352 G. Ceder, K.A. Persson, Commentary: The Materials Project: A materials genome approach to
353 accelerating materials innovation, APL Materials. 1 (2013) 011002. doi:10.1063/1.4812323.
- 354 [24] G.T. Furukawa, T.B. Douglas, W.G. Saba, A.C. Victor, Heat Capacity and Enthalpy Measurements
355 on Aluminum Carbide (Al₄C₃) From 15 to 1173 OK. Thermodynamic Properties From 0 to 2000
356 °K, JOURNAL OF RESEARCH of the National Bureau of Standards-A. Physics and Chemistry. 69A
357 (1965) 423–438.
- 358 [25] M.W. Chase, National Institute of Standards and Technology (U.S.), eds., NIST-JANAF
359 thermochemical tables, 4th ed, American Chemical Society ; American Institute of Physics for
360 the National Institute of Standards and Technology, Washington, DC : New York, 1998.
- 361 [26] I.G. Buda, C. Lane, B. Barbiellini, A. Ruzsinszky, J. Sun, A. Bansil, Characterization of Thin Film
362 Materials using SCAN meta-GGA, an Accurate Nonempirical Density Functional, Scientific
363 Reports. 7 (2017). doi:10.1038/srep44766.
- 364 [27] J. Sun, A. Ruzsinszky, J.P. Perdew, Strongly Constrained and Appropriately Normed Semilocal
365 Density Functional, Physical Review Letters. 115 (2015). doi:10.1103/PhysRevLett.115.036402.
- 366 [28] G. Höhne, W. Hemminger, H.-J. Flammersheim, Differential scanning calorimetry, Springer,
367 Heidelberg; New York, 2010.
- 368 [29] P. Hohenberg, W. Kohn, Inhomogeneous Electron Gas, Physical Review. 136 (1964) B864–B871.
369 doi:10.1103/PhysRev.136.B864.
- 370 [30] W. Kohn, L.J. Sham, Self-Consistent Equations Including Exchange and Correlation Effects,
371 Physical Review. 140 (1965) A1133–A1138. doi:10.1103/PhysRev.140.A1133.
- 372 [31] G. Kresse, J. Furthmüller, Efficient iterative schemes for *ab initio* total-energy calculations using
373 a plane-wave basis set, Physical Review B. 54 (1996) 11169–11186.
374 doi:10.1103/PhysRevB.54.11169.
- 375 [32] G. Kresse, D. Joubert, From ultrasoft pseudopotentials to the projector augmented-wave
376 method, Physical Review B. 59 (1999) 1758–1775. doi:10.1103/PhysRevB.59.1758.

- 377 [33] J. Klimeš, D.R. Bowler, A. Michaelides, Van der Waals density functionals applied to solids,
378 Physical Review B. 83 (2011). doi:10.1103/PhysRevB.83.195131.
- 379 [34] J. Klimeš, D.R. Bowler, A. Michaelides, Chemical accuracy for the van der Waals density
380 functional, Journal of Physics: Condensed Matter. 22 (2010) 022201. doi:10.1088/0953-
381 8984/22/2/022201.
- 382 [35] H.J. Monkhorst, J.D. Pack, Special points for Brillouin-zone integrations, Physical Review B. 13
383 (1976) 5188–5192. doi:10.1103/PhysRevB.13.5188.
- 384 [36] P.E. Blöchl, O. Jepsen, O.K. Andersen, Improved tetrahedron method for Brillouin-zone
385 integrations, Physical Review B. 49 (1994) 16223–16233. doi:10.1103/PhysRevB.49.16223.
- 386 [37] A. Togo, I. Tanaka, First principles phonon calculations in materials science, Scripta Materialia.
387 108 (2015) 1–5. doi:10.1016/j.scriptamat.2015.07.021.
- 388 [38] P. Benigni, G. Mikaelian, R. Pothin, A. Berche, R.M. Ayrat, J.C. Tedenac, P. Jund, J. Rogez,
389 Measurement of the heat capacity of ZnSb by DSC between 300 and 673 K, Calphad. 55 (2016)
390 238–242. doi:10.1016/j.calphad.2016.09.008.
- 391 [39] G.A. Uriano, Standard Reference Material 720 Synthetic Sapphire (α -Al₂O₃), National Bureau of
392 Standards Certificate. (1982).
- 393 [40] J.B. Nelson, D.P. Riley, The thermal expansion of graphite from 15C to 800C: Part I.
394 Experimental., Proceedings of the Physical Society. 57 (1945).
- 395 [41] Y. Baskin, L. Meyer, Lattice Constants of Graphite at Low Temperatures, Physical Review. 100
396 (1955) 544–544. doi:10.1103/PhysRev.100.544.
- 397 [42] P. Trucano, R. Chen, Structure of graphite by neutron diffraction, Nature. 258 (1975) 136–137.
398 doi:10.1038/258136a0.
- 399 [43] Y.X. Zhao, I.L. Spain, X-ray diffraction data for graphite to 20 GPa, Physical Review B. 40 (1989)
400 993–997. doi:10.1103/PhysRevB.40.993.
- 401 [44] J.Y. Howe, C.J. Rawn, L.E. Jones, H. Ow, Improved crystallographic data for graphite, Powder
402 Diffraction. 18 (2003) 150–154. doi:10.1154/1.1536926.
- 403 [45] D.P. Riley, Lattice Constant of Diamond and the C–C Single Bond, Nature. 153 (1944) 587–588.
404 doi:10.1038/153587b0.
- 405 [46] M.E. Straumanis, E.Z. Aka, Precision Determination of Lattice Parameter, Coefficient of Thermal
406 Expansion and Atomic Weight of Carbon in Diamond ¹, Journal of the American Chemical
407 Society. 73 (1951) 5643–5646. doi:10.1021/ja01156a043.
- 408 [47] T. Hom, W. Kisztenik, B. Post, Accurate lattice constants from multiple reflection measurements.
409 II. Lattice constants of germanium silicon, and diamond, Journal of Applied Crystallography. 8
410 (1975) 457–458. doi:10.1107/S0021889875010965.
- 411 [48] A. Zunger, Self-consistent LCAO calculation of the electronic properties of graphite. I. The
412 regular graphite lattice, Physical Review B. 17 (1978) 626–641. doi:10.1103/PhysRevB.17.626.
- 413 [49] M.T. Yin, M.L. Cohen, Ground-state properties of diamond, Physical Review B. 24 (1981) 6121–
414 6124. doi:10.1103/PhysRevB.24.6121.
- 415 [50] C. Kittel, Introduction to solid state physics, 7. ed, Wiley, New York, NY, 1996.
- 416 [51] M. v. Stackelberg, E. Schnorrenberg, Die Struktur des Aluminiumcarbids Al₄C₃, Zeitschrift Für
417 Physikalische Chemie. 27B (1934). doi:10.1515/zpch-1934-0107.
- 418 [52] J.H. Cox, L.M. Pidgeon, THE X-RAY DIFFRACTION PATTERNS OF ALUMINUM CARBIDE Al₄C₃
419 AND ALUMINUM OXYCARBIDE Al₄O₄C, Canadian Journal of Chemistry. 41 (1963) 1414–1416.
420 doi:10.1139/v63-192.
- 421 [53] G.A. Jeffrey, V. Wu, The structure of the aluminum carbonitrides. II, Acta Crystallographica. 20
422 (1966) 538–547. doi:10.1107/S0365110X66001208.
- 423 [54] T.M. Gesing, W. Jeitschko, The Crystal Structure and Chemical Properties of U₂Al₃C₄ and
424 Structure Refinement of Al₄C₃, Zeitschrift Für Naturforschung B. 50 (1995) 196–200.
425 doi:10.1515/znb-1995-0206.
- 426 [55] D.V. Suetin, I.R. Shein, A.L. Ivanovskii, Structural, elastic and electronic properties and
427 formation energies for hexagonal (W_{0.5}Al_{0.5})C in comparison with binary carbides WC and

- 428 Al₄C₃ from first-principles calculations, *Physica B: Condensed Matter*. 403 (2008) 2654–2661.
429 doi:10.1016/j.physb.2008.01.045.
- 430 [56] L. Sun, Y. Gao, K. Yoshida, T. Yano, W. Wang, Prediction on structural, mechanical and thermal
431 properties of Al₄SiC₄, Al₄C₃ and 4H-SiC under high pressure by first-principles calculation,
432 *Modern Physics Letters B*. 31 (2017) 1750080. doi:10.1142/S0217984917500804.
- 433 [57] W.G. Saba, G.T. Furukawa, Aluminium carbide. Measurements of the low-temperature heat
434 capacity and correlation of the results with high-temperature enthalpy data, NBS Report 7587.
435 (1962).
- 436 [58] F.D. Rossini, R.S. Jessup, Heat and free energy of formation of carbon dioxide, and of the
437 transition between graphite and diamond, *Journal of Research of the National Bureau of*
438 *Standards*. 21 (1938) 491–513.
- 439 [59] O.J. Kleppa, K.C. Hong, New applications of high-temperature solution calorimetry 1. Enthalpy
440 of the diamond-to-graphite transformation and enthalpy of formation of Mn₅C₂ at 1320 K, *The*
441 *Journal of Chemical Thermodynamics*. 10 (1978) 243–248. doi:10.1016/0021-9614(78)90020-4.
- 442 [60] R. Hultgren, P.D. Desai, D.T. Hawkins, M. Gleiser, K.K. Kelley, D.D. Wagman, Selected Values of
443 the Thermodynamic Properties of the Elements, ASM, Metals Park, OH, 1973.
- 444 [61] V.P. Glushko, *Thermal Constants of Substances*, Nauka, Moscow. (1965).
- 445 [62] E.B. Isaacs, C. Wolverton, Performance of the strongly constrained and appropriately normed
446 density functional for solid-state materials, *Physical Review Materials*, 2(6)(2018) 063801. doi:
447 10.1103/PhysRevMaterials.2.063801

448